

Blind Identification of the Central Aortic Pressure Waveform from Multiple Peripheral Arterial Pressure Waveforms

Gokul Swamy, Qi Ling, Tongtong Li, *Member, IEEE*, Ramakrishna Mukkamala, *Member, IEEE*

Abstract—We introduce a blind identification technique to reconstruct the clinically more relevant central aortic pressure waveform from multiple less invasively measured peripheral arterial pressure waveforms. We conducted initial testing of the technique in two swine in which peripheral arterial pressure waveforms from the femoral and radial arteries and reference central aortic pressure were simultaneously measured during diverse hemodynamic conditions. We report an overall error between the estimated and measured central aortic pressure waveforms of 4.8%. Potential clinical applications of the technique may include critical care monitoring with respect to invasive catheter systems and emergency and home monitoring with respect to non-invasive arterial pressure transducers.

I. INTRODUCTION

As the arterial pressure wave traverses from the central aorta to smaller peripheral arteries, its contour becomes significantly distorted due to complex wave reflections in the distributed arterial tree [1]. For example, both systolic pressure and pulse pressure usually become amplified, with the extent of the amplification dependent on the particular peripheral site and state of the arterial tree [2]. Thus, it is the systolic and diastolic pressures measured specifically in the central aorta that truly reflect cardiac afterload and perfusion [3]. Perhaps, as a result, central measurements of systolic pressure and pulse pressure have been shown to be superior in predicting outcome than corresponding measurements made in more peripheral arteries [4][5]. Moreover, central aortic pressure is not significantly complicated by the wave phenomena [6][7]. Thus, the entire central aortic pressure waveform often reveals the cardiac ejection time through the dicrotic notch (which is obscured by wave reflections in peripheral arterial pressure waveforms) [8] and may be fitted to relatively simple models in order to accurately estimate other clinically important hemodynamic variables such as beat-to-beat proportional stroke volume [6].

The measurement of the central aortic pressure waveform usually involves introducing a catheter in a peripheral artery

and guiding the catheter against the flowing blood to the central aorta. However, placement of an aortic catheter is not commonly performed in clinical practice [3] because of the risk of blood clot formation and embolization.

On the other hand, related, but distorted, peripheral arterial pressure waveforms may be measured less invasively and more safely via placement of a catheter in a distal artery, especially the radial or femoral artery. Indeed, radial and femoral artery catheterizations are routinely performed in clinical practice [9]. Moreover, totally non-invasive methods are commercially available to continuously measure peripheral arterial pressure based on finger-cuff photoplethysmography [10] and applanation tonometry [11].

Several techniques have therefore been recently introduced to mathematically derive the clinically more relevant central aortic pressure waveform from less invasively measured peripheral arterial pressure waveforms. Most of these techniques have generally involved 1) initially obtaining simultaneous measurements of central aortic and peripheral arterial pressure waveforms in a group of subjects, 2) estimating a group-averaged transfer function relating the measured peripheral arterial pressure to the measured central aortic pressure, and 3) subsequently applying this generalized transfer function to measured peripheral arterial pressure in order to predict the unobserved central aortic pressure waveform [2][3][8][12]. The principal assumption underlying these techniques is that arterial tree properties are relatively constant over all time and between all individuals. Because of known inter-subject and temporal variability of the arterial tree, a few methods have been more recently proposed towards partial individualization of the transfer function relating peripheral arterial pressure to central aortic pressure using a model-based approach [13][14].

It would be desirable to be able to estimate the central aortic pressure waveform from peripheral arterial pressure waveforms in an entirely data specific manner. One possible way to do so is with recently developed multi-channel blind system identification techniques in which the outputs of a single input, multi-output system are analyzed so as to reconstruct the common input [15][16]. To our knowledge, the study by McCombie et al. represents the only application of multi-channel blind system identification to the field of hemodynamic monitoring [17]. However, their study was specifically designed to estimate the morphology of the aortic flow from peripheral arterial measurements.

In this study, we introduce a blind identification technique to reconstruct the absolute central aortic pressure waveform from multiple peripheral arterial pressure waveform measurements. We then demonstrate the validity of the

Manuscript received April 3, 2006. This work was supported by the NIBIB Grant EB-004444 and an award from the AHA.

G. Swamy is with the Department of Electrical and Computer Engineering, East Lansing, MI 48824 USA (email: swamygok@msu.edu).

Q. Ling is with the Department of Electrical and Computer Engineering, East Lansing, MI 48824 USA (email: lingqi@msu.edu).

T. Li is with the Department of Electrical and Computer Engineering, East Lansing, MI 48824 USA (email: tongli@egr.msu.edu).

R. Mukkamala is with the Department of Electrical and Computer Engineering, East Lansing, MI 48824 USA (phone: 517-353-3120; fax: 517-353-1980; e-mail: rama@egr.msu.edu).

technique with respect to two swine in which femoral and radial arterial pressure waveforms and a reference central aortic pressure waveform were simultaneously measured during diverse hemodynamic interventions.

II. BLIND IDENTIFICATION TECHNIQUE

Our technique for estimating the central aortic pressure waveform is generally implemented according to the following four steps: 1) modeling the measured peripheral arterial pressure waveforms as outputs of distinct channels driven by the common central aortic pressure input; 2) applying multi-channel blind system identification to the measured waveforms to estimate the channels of the model to within an arbitrary scale factor; 3) applying the inverse of the estimated channels to the measured waveforms to reconstruct the central aortic pressure waveform to within an arbitrary scale factor; and 4) scaling the reconstructed waveform to absolute central aortic pressure based on physiologic knowledge. Each of these steps is specifically implemented as described below.

First, the relationship amongst the pressures at different arterial tree sites is modeled as a single-input, multi-output system as shown in Fig. 1. More specifically, the m outputs of the system ($p_{pi}(t)$, $1 \leq i \leq m$, where $m > 1$) correspond to m measured and sampled peripheral arterial pressure waveforms, while the common input ($p_{ca}(t)$) represents the unmeasured and likewise sampled central aortic pressure waveform. Each of the discrete-time channels coupling the common input to each distinct output characterizes the dynamic properties of a different arterial tree path.

The assumptions underlying the model of Fig. 1 are as follows. The channels are assumed to be linear and time-invariant (LTI) over each time interval of the subsequent mathematical analysis (1 min intervals as described below). Over such short time intervals, the arterial tree is usually operating in near steady-state conditions in which the statistical properties of the pressure waveforms vary little over time. Such steady-state conditions clearly justify a time-invariance approximation while also supporting a linearity approximation (see [17] and references therein). The LTI channels are further assumed to be well approximated with finite impulse responses (FIRs; $h_i(t)$, $1 \leq i \leq m$, $0 \leq t \leq L$, where L is the maximum order of the FIRs). This assumption is well justified, since pressure waveforms from distinct arterial sites only differ significantly in terms of their high frequency detail while being quite similar at lower frequencies [7][18]. Thus, the dynamics of each of the channels are fast and effectively vanish within ~ 0.5 sec [19]. The FIRs are also assumed to be coprime (*i.e.*, have no common zeros) with each other, which is necessary for the subsequent application of multi-channel blind system identification and signal detection [15][16]. This assumption may be more valid for some groups of peripheral arterial pressure waveforms than others. Finally, the central aortic pressure waveform input is assumed to be persistently exciting of high enough order (*i.e.*, containing at least as many frequency components as the number of parameters needed to characterize all of the channels), which is also

necessary for the subsequent application of multi-channel blind system identification [16]. Since the channel dynamics are short in duration, the number of parameters to be estimated may be small enough to satisfy this assumption.

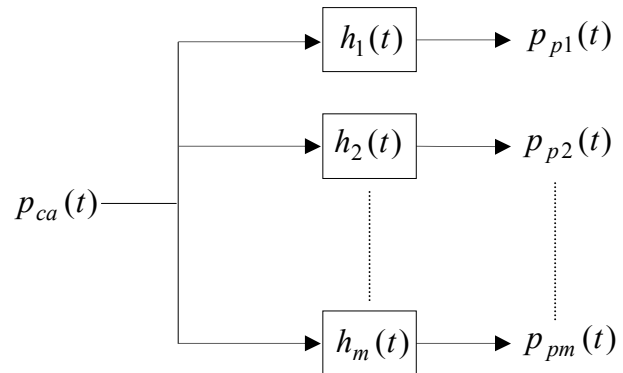


Fig. 1. Single-input, multi-output model of the relationship of the pressures at different sites in the arterial tree. The outputs ($p_{pi}(t)$, $1 \leq i \leq m$) correspond to measured peripheral arterial pressure waveforms, while the common input ($p_{ca}(t)$) corresponds to an unmeasured central aortic pressure waveform. Each channel ($h_i(t)$, $1 \leq i \leq m$) coupling the common input to each distinct output represents the dynamic properties of a different arterial tree path.

Second, the m FIRs $h_i(t)$ in Fig. 1 are estimated to within an arbitrary scale factor from the m measured outputs $p_{pi}(t)$ based on the cross relations between pairs of measured outputs as described in [16]. Below, we briefly review this multi-channel blind system identification technique when $m = 2$ for the sake of simplicity. The cross relation between the two measured and sampled outputs is specifically given as follows:

$$\sum_{k=0}^{L-1} h_1(k) p_{p2}(t-k) - \sum_{k=0}^{L-1} h_2(k) p_{p1}(t-k) = e(t), \quad t \in [L-1, N-1], \quad (1)$$

where $e(t)$ accounts for measurement noise and/or modeling error, and N represents the number of available output samples. Equation (1) may be expressed in matrix form by stacking each individual equation for a given t , one on top of the other, as follows:

$$\underbrace{\begin{bmatrix} \mathbf{P}_{p2} & -\mathbf{P}_{p1} \end{bmatrix}}_{\mathbf{P}} \underbrace{\begin{bmatrix} \mathbf{h}_1 \\ \mathbf{h}_2 \end{bmatrix}}_{\mathbf{h}} = \mathbf{e}. \quad (2)$$

Here, \mathbf{P}_{p1} and \mathbf{P}_{p2} are $[(N-L+1) \times L]$ Hankel matrices comprising the respective measured output samples, \mathbf{h}_1 and \mathbf{h}_2 are $[L \times 1]$ vectors including the parameters of the two respective FIRs, and \mathbf{e} is an $[(N-L+1) \times 1]$ vector of the noise samples. For a fixed channel order L , the vector \mathbf{h} is estimated to a certain non-trivial constraint by minimizing the energy in the vector \mathbf{e} . This optimization problem is specifically solved by selecting the eigenvector associated with the smallest eigenvalue in the matrix $\mathbf{P}^T \mathbf{P}$ as a unit-energy estimate of the vector \mathbf{h} . The channel order L is determined by minimizing the Minimum Description Length (MDL) criterion over a range of candidate values of L [20].

Third, the common input $p_{ca}(t)$ in Fig. 1 is determined to within an arbitrary scale factor from the m FIRs $h_i(t)$ (in the estimated vector \mathbf{h}) and the m measured outputs $p_{pi}(t)$ through multi-channel least squares deconvolution as described in [15]. Below, we likewise briefly review this technique when $m = 2$. The two measured outputs may be expressed in terms of their common input via the convolution sum as follows:

$$p_{pi}(t) = \sum_{k=0}^{L-1} h_i(k) p_{ca}(t-k) + n_i(t) \quad (3)$$

where $n_i(t)$ accounts for any noise. Equation (3) may be expressed in matrix form by stacking each individual equation for a given output and t , one on top of the other, as follows:

$$\begin{bmatrix} \mathbf{p}_{p1} \\ \mathbf{p}_{p2} \end{bmatrix} = \begin{bmatrix} \mathbf{H}_1 \\ \mathbf{H}_2 \end{bmatrix} \mathbf{p}_{ca} + \begin{bmatrix} \mathbf{n}_1 \\ \mathbf{n}_2 \end{bmatrix}. \quad (4)$$

$\mathbf{p}_p \qquad \mathbf{H} \qquad \mathbf{n}$

Here, \mathbf{p}_{p1} and \mathbf{p}_{p2} are $[N \times 1]$ vectors of the respective measured output samples, \mathbf{H}_1 and \mathbf{H}_2 are the $[N \times (N+L)]$ Sylvester matrices including the estimated parameters of the respective FIRs, \mathbf{p}_{ca} is a $[(N+L) \times 1]$ vector of unmeasured common input samples, and \mathbf{n} is a $[N \times 1]$ vector of the noise samples. The vector \mathbf{p}_{ca} is then estimated to within an arbitrary scale factor by minimizing the energy in the vector \mathbf{n} . This optimization problem is specifically solved in closed-form using the linear least squares solution as follows:

$$\mathbf{p}_{ca} = (\mathbf{H}^T \mathbf{H})^{-1} \mathbf{H}^T \mathbf{p}_p. \quad (5)$$

Following the deconvolution, the reconstructed input is lowpass filtered with a cutoff frequency equal to 5 Hz.

Fourth, the reconstructed central aortic pressure waveform above is scaled to have a mean value equal to that of the measured peripheral arterial pressure. This scaling step is well justified, since the paths from the central aorta to peripheral arteries offer very little resistance to blood flow due to Poiseuille's law [7]. Note that the reconstructed absolute central aortic pressure waveform will be slightly delayed with respect to the true central aortic pressure waveform, because the time delay shared by the channels in Fig. 1 cannot be identified with blind identification [17]. However, this delay, which is usually < 0.1 sec, is irrelevant for most clinical applications.

III. METHODS

A. Experimental Procedures

The hemodynamic data utilized here to initially evaluate the blind identification technique were originally collected to address different specific aims, and the materials and methods are presented in detail elsewhere [18]. We briefly describe below the most basic aspects of the experimental procedures that were relevant to the present study. All procedures were reviewed and approved by the MIT Committee on Animal Care.

Two swine (~ 30 kg) were studied as follows. After

induction of general anesthesia, instrumentation was installed including catheters in the femoral artery for femoral arterial pressure, an artery as distal as possible to the brachial artery for radial arterial pressure, and the descending aorta (approximately 20-25 cm from the aortic root) via the opposite femoral artery for reference central aortic pressure. The pressures were then continuously recorded and sampled at 250 Hz during the administration of isoproterenol, esmolol, phenylephrine, nitroglycerin, and acetylcholine as well as the infusion of volume in order to vary the hemodynamic conditions over a wide range (see Table I).

B. Data Analysis

The technique was applied to 1 min segments of the femoral and radial arterial pressure waveforms from each swine. To quantitatively assess the overall performance of the technique, the root-mean-squared-normalized-error (RMSNE) between all of the estimated and corresponding measured central aortic pressure waveform segments was computed. For comparison, the RMSNE between all of the peripheral arterial pressure waveform segments and corresponding measured central aortic pressure waveform segments was also computed.

IV. RESULTS

Table I summarizes the results of the experimental evaluation of the technique in the two swine. This table indicates that the overall RMSNE between the estimated and reference central aortic pressure waveform segments was 4.8%. For comparison, the average overall RMSNE between the peripheral arterial pressure waveform segments and reference central aortic pressure waveform segments was 11.8%. Thus, the technique was effectively able to reduce the wave distortion in the peripheral arterial pressure waveform segments by 59.3%. Fig. 2 provides an example illustrating significant differences between peripheral arterial pressure waveform segments (short-dashed and long-dashed) and the corresponding measured central aortic pressure waveform segment (solid), while Fig. 3 shows the central aortic pressure waveform segment estimated from these peripheral arterial pressure waveform segments (short-dashed) along with the reference central aortic pressure waveform segment (solid).

V. SUMMARY AND CONCLUSIONS

In summary, we have introduced a blind identification technique to reconstruct the clinically more relevant central aortic pressure waveform from multiple less invasively measured peripheral arterial pressure waveforms. We have applied the technique to femoral and radial arterial pressure waveforms from two swine over a wide hemodynamic range and found that the technique was able to effectively reduce the wave distortion in the peripheral arterial pressure waveforms by 59.3%. In the future, we plan to further develop the technique and determine the optimal sites in the

arterial tree for which the peripheral arterial pressure waveforms should be measured. Potential applications of the technique may include critical care monitoring with respect to invasive catheter systems as well as emergency and home monitoring with respect to non-invasive arterial pressure transducers.

TABLE I
SUMMARY OF THE EXPERIMENTAL EVALUATION OF THE BLIND IDENTIFICATION TECHNIQUE.

ANIMAL	MAP RANGE [MMHG]	HR RANGE [BPM]	CAP RMSNE [%]	FAP RMSNE [%]	RAP RMSNE [%]
1	57 - 143	99 - 223	5.3	15.7	7.5
2	44 - 114	91 - 243	4.5	11.8	11.6
TOTAL	44 - 143	91 - 243	4.8	13.2	10.4

MAP is mean arterial pressure; HR, heart rate; CAP, central aortic pressure; FAP, femoral arterial pressure; RAP, radial arterial pressure; and RMSNE, root-mean-squared-normalized error.

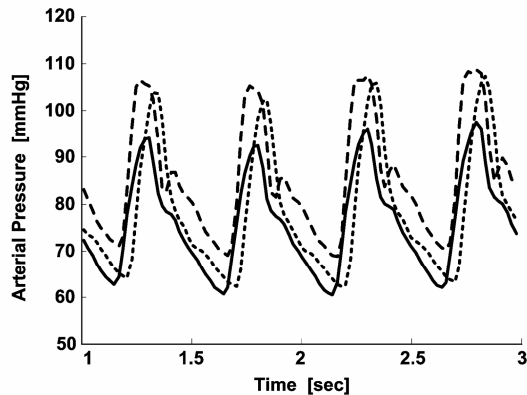


Fig. 2. Example of the measured central aortic pressure (solid), femoral arterial pressure (long-dashed), and radial arterial pressure (short-dashed) waveform segments from one of the swine.

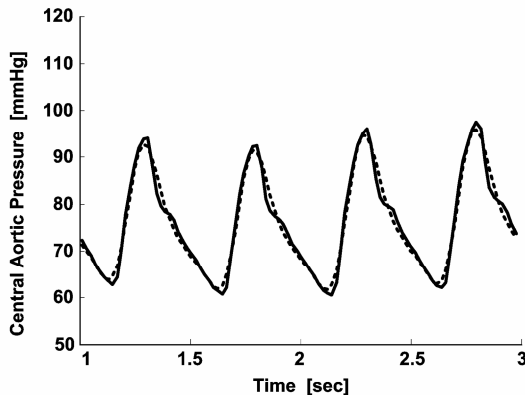


Fig. 3. Example of an estimated (dashed) and measured (solid) central aortic pressure waveform segment. The estimated segment was obtained by applying the blind identification technique to the two peripheral arterial pressure waveform segments in Fig. 2.

REFERENCES

[1] M. F. O'Rourke and T. Yaginuma, "Wave reflections and the arterial pulse," *Arch. Intern. Med.*, vol. 144, pp. 366-371, 1984.
 [2] S. Soderstrom, G. Nyberg, M. F. O'Rourke, J. Sellgren, and J. Ponten, "Can a clinically useful aortic pressure wave be derived from

a radial pressure wave?," *Br. J. Anaesth.*, vol. 88, no. 4, pp. 481-488, 2002.
 [3] C. H. Chen, E. Nevo, B. Fetics, P. H. Pak, F. C. Yin, W. L. Maughan, and D. A. Kass, "Estimation of central aortic pressure waveform by mathematical transformation of radial tonometry pressure. Validation of generalized transfer function," *Circulation*, vol. 95, no. 7, pp. 1827-1836, 1997.
 [4] M. E. Safar, J. Blacher, B. Pannier, A. P. Guerin, S. J. Marchais, P. Guyonvarc'h, and G. M. London, "Central pulse pressure and mortality in end-stage renal disease," *Hypertension*, vol. 39, pp. 735-738, 2002.
 [5] T. K. Waddell, A. M. Dart, T. L. Medley, J. D. Cameron, and B. A. Kingwell, "Carotid pressure is a better predictor of coronary artery disease severity than brachial pressure," *Hypertension*, vol. 38, pp. 927-931, 2001.
 [6] M. J. Bourgeois, B. K. Gilbert, G. von Bernuth, and E. H. Wood, "Continuous determination of beat-to-beat stroke volume from aortic pressure pulses in the dog," *Circ. Res.*, vol. 39, no. 1, pp. 15-24, 1976.
 [7] A. Noordergraaf. *Circulatory System Dynamics*. New York: Academic Press, 1978.
 [8] B. Fetics, E. Nevo, C. H. Chen, and D. A. Kass, "Parametric model derivation of transfer function for noninvasive estimation of aortic pressure by radial tonometry," *IEEE Trans. Biomed. Eng.*, vol. 46, no. 6, pp. 698-706, 1999.
 [9] P. L. Marino. *The ICU Book*. Baltimore: Lippincott Williams & Wilkins, 1998.
 [10] B. P. M. Imholz, W. Wieling, G. A. van Montfrans, and K. H. Wesseling, "Fifteen years experience with finger arterial pressure monitoring: assessment of the technology," *Cardiovasc. Res.*, vol. 38, pp. 605-616, 1998.
 [11] T. Kenner, "ABP and its measurement," *Basic Res. Cardiol.*, vol. 83, no. 2, pp. 107-121, 1988.
 [12] M. Karamanoglu, M. F. O'Rourke, A. P. Avolio, and R. P. Kelly, "An analysis of the relationship between central aortic and peripheral upper limb pressure waves in man," *Eur. Heart J.*, vol. 14, pp. 160-167, 1993.
 [13] M. Karamanoglu and M. P. Feneley, "On-line synthesis of the human ascending aortic pressure pulse from the finger pulse," *Hypertension*, vol. 30, pp. 1416-1424, 1997.
 [14] M. Sugimachi, T. Shishido, K. Miyatake, and K. Sunagawa, "A new model-based method of reconstructing central aortic pressure from peripheral arterial pressure," *Jpn. J. Physiol.*, vol. 51, no. 2, pp. 217-222, 2001.
 [15] K. Abed-Meraim, W. Qiu, and Y. Hua, "Blind system identification," *Proc. of IEEE*, vol. 85, no. 12, pp. 1310-1332, 1997.
 [16] G. Xu, H. Liu, L. Tong, and T. Kailath, "A least-squares approach to blind channel identification," *IEEE Trans. Signal Processing*, vol. 43, no. 12, pp. 2982-2993, 1995.
 [17] D. B. McCombie, A. T. Reisner, and H. H. Asada, "Laguerre-model blind system identification: cardiovascular dynamics estimated from multiple peripheral circulatory signals," *IEEE Trans. Biomed. Eng.*, vol. 52, no. 11, pp. 1889-1901, 2005.
 [18] R. Mukkamala, A. T. Reisner, H. M. Hojman, R. G. Mark, and R. J. Cohen, "Continuous cardiac output monitoring by peripheral blood pressure waveform analysis," *IEEE Trans. Biomed. Eng.*, vol. 53, no. 3, pp. 459-467, 2006.
 [19] Y. Zhang, H. H. Asada, and A. T. Reisner, "Noninvasive cardiac output monitoring based on multi-channel blind system id and modal decomposition," *Proc. 2nd Joint EMBS/BMES Conf.*, vol. 1, pp. 218-219, 2002.
 [20] L. Ljung. *System Identification: Theory for the User*. Englewood Cliffs: PTR Prentice Hall, 1987.